Performance Analysis of STAR-RIS Enhanced CoMP-NOMA Multi-Cell Networks

Muhammad Umer*, Muhammad Ahmed Mohsin*, Syed Ali Hassan*, Haejoon Jung†, and Haris Pervaiz‡

*School of Electrical Engineering and Computer Science (SEECS), NUST, Pakistan
†Department of Electronics and Information Convergence Engineering, Kyung Hee University, Republic of Korea
‡School of Computing and Communications, Lancaster University, UK
Email: {mumer.bee20seecs, mmohsin.bee20seecs, ali.hassan}@seecs.edu.pk,
haejoonjung@khu.ac.kr, h.b.pervaiz@lancaster.ac.uk

Abstract—In this paper, we present a novel approach to enhance data rates in a multi-cell network through the simultaneous utilization of reconfigurable intelligent surfaces (STAR-RISs), and non-orthogonal multiple access (NOMA) coordinated multi-point transmission (CoMP). By strategically deploying STAR-RISs, the data rate for cell-center and cell-edge users is improved, achieved through exhaustive computation to optimize the system's performance. The study conducts a comparative resource allocation analysis to maximize data rates for cell-edge and cell-center users. Additionally, the investigation explores the effects of CoMP and non-CoMP systems on the outage conditions and data rates, offering valuable insights into future wireless communication system design and optimization.

Index Terms—NOMA, CoMP, STAR-RIS

I. INTRODUCTION

Reconfigurable Intelligent Surfaces (RISs) offer a promising solution for enhancing spectral efficiency (SE) and coverage in sixth-generation (6G) wireless networks [1], [2]. They are essentially a 2-D metasurface equipped with low-cost, eco-friendly passive elements. Being passive in nature, these devices can enhance signal coverage by adjusting both phase and amplitude so that the signals are combined constructively at the desired receiver. Their passive behavior promotes green Internet in digital ecosystems, providing higher data rates and spectral efficiency while being cost-effective. RIS only passively recycles signals that are already part of the wireless network. Despite its advantage of improving the data rates and signal coverage, these surfaces impose a problem called the half-space problem, which requires that the impinging signal and the user must be located on the same side of RIS, introducing additional constraints to the system, as in [3].

To overcome this limitation, recent research in developing metasurfaces and advanced fabrication technologies led to a novel idea of Simultaneously Transmitting and Reflecting Reconfigurable Intelligent Surfaces (STAR-RIS), which divides its elements so that some take part in reflection and the rest in transmission. STAR-RIS can enhance the non-line-of-sight coverage of the impinging signal by providing a virtual line-of-sight path by establishing links to both surfaces, which can solve the half-space problem.

The quest for improved performance in cellular networks has prompted the deployment of numerous low-power, cost-effective, and compact (BSs). However, this proliferation has given rise to a formidable cross-tier inter-cell interference (ICI) obstacle, which hinders further advancements. Furthermore, the substantial power consumption resulting from the dense BS deployment presents a pressing challenge.

Coordinated multi-point (CoMP) techniques have emerged as a promising solution to address these issues. Through high-speed fronthaul links and the sharing of channel state information (CSI) among BSs, CoMP networks allow for the mitigation of ICI and the consequent enhancement of overall network performance. CoMP was introduced by the Long Term Evolution Advanced (LTE-A) by the third generation partnership project (3GPP) and is a crucial component for 5G communications. Coordination among all the BSs is complex due to inaccurate CSI, additional synchronization across cells, and additional signal processing. Making clusters for CoMP wireless systems is also an optimization problem for future wireless networks.

On the other hand, multiple access techniques have been established to increase the spectral efficiency of wireless systems, and non-orthogonal multiple access (NOMA) is one of them. The power-domain NOMA superposes multiple users in the power domain. However, the downlink signal could be transmitted based on any other baseline in the LTE system.

In this paper, we consider a STAR-RIS enhanced CoMP-NOMA network and present a detailed analysis of the achievable rates of cellular users. The main contributions of this paper can be summarized as follows.

- A novel model for the joint utilization of STAR-RISs and CoMP-NOMA to enhance the system performance in a multi-cell network. By strategically deploying STAR-RISs, we are able to improve the network coverage and outage conditions of the cell-edge user.
- Investigating the impact of CoMP and non-CoMP systems on diverse performance metrics, we demonstrate the superiority of strategically placed and optimized STAR-RISs over conventional systems.
- Investigating the impact of strategically assigning STAR-RIS elements to BSs based on the channel conditions, and optimizing amplitude adjustments for transmission and reflection regions, on the achievable network sum-rate.
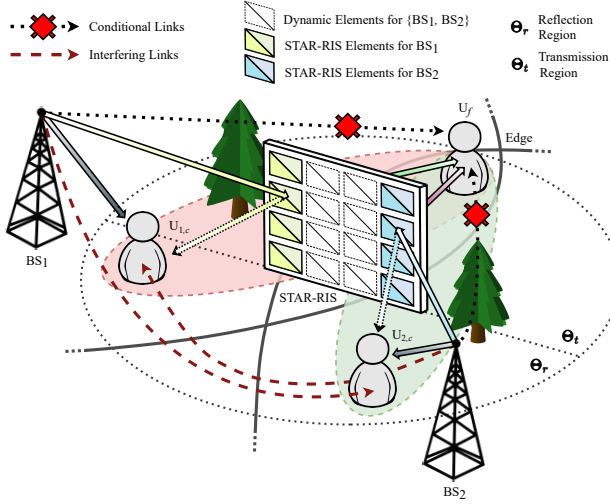
Fig. 1. An illustration of STAR-RIS aided coordinated NOMA cluster.

II. SYSTEM MODEL

A. System Layout

As shown in Fig. 1, we consider a narrow-band two-cell CoMP NOMA downlink communication system operating over frequency-flat channels aided by a STAR-RIS comprising K elements strategically positioned at the intersection of the cells. Let the index sets be defined as $\mathcal{I} = \{1, 2\}$ for the two BSs, $\mathcal{C} = \{1, 2, \dots, C\}$ for the cell-center users, and $\mathcal{F} = \{1, 2, \dots, F\}$ for the cell-edge users, where C, and F represent the cardinality of $\mathcal{C}$, and $\mathcal{F}$, respectively. Additionally, let $\mathcal{U} = \{\mathcal{M} \cup \mathcal{N} \cup \mathcal{F}\}$ be the set of all users in the system. For simplicity, we only focus on the typical scenario, where each BS is equipped with a single antenna, establishing communication links with one single-antenna cell-center user and one single-antenna cell-edge user. Thus, in this context, we have $M = 1$, $N = 1$, and $F = 1$. In addition, $\forall c \in \mathcal{C}$, $\forall f \in \mathcal{F}$, U_c is placed in the reflection region $\mathbf{\Theta_r}$, while U_f is placed in the transmission region $\mathbf{\Theta_t}$ of the STAR-RIS.

The BSs employ power-domain NOMA techniques to communicate with the users. Specifically, $\forall i \in \mathcal{I}, c \in \mathcal{C}$, and $f \in \mathcal{F}$, BS_i forms the NOMA pair $(U_{i,c}, U_f)$, where $U_{i,c}$ is the cell-center user of BS_i. Consequently, the U_f is part of two NOMA pairs, each cluster served by a different base station. To mitigate the strong ICI experienced by U_f, CoMP is adopted between the two BSs. In addition, it is assumed that the BSs are connected to a central processing unit (CPU) via high-speed fronthaul links, facilitating seamless information sharing and coordinated transmissions among them.

In this paper, perfect CSI is assumed to be available at the BSs. While this is a challenging assumption in practice, recent advances in channel estimation techniques for RIS-enabled wireless networks have shown that it is possible to achieve accurate CSI [3]–[5] with a reasonable amount of overhead. These estimation methods can also be applied to STAR-RISs, but are beyond the scope of this work.

B. Channel Model

For each communication link in the system, we take into account both large-scale fading and small-scale fading effects. Due to the relatively large propagation distances and the scattering effect of the links between B_i and U_u, $\forall i \in \mathcal{I}$ and $u \in \mathcal{U}$, the channels are assumed to follow Rayleigh fading, expressed as:

$$\mathbf{h}_{i,u} = \sqrt{\frac{\rho_o}{PL(d_{i,u})}} \mathbf{v}_{i,u} \tag{1}$$

where $\mathbf{v}_{i,u}$ is a complex Gaussian random variable that follows a Rayleigh distribution with zero mean and unit variance, ρ_o is the reference path-loss at a distance of 1 m, $PL(d_{i,u})$ is the large scale path-loss, modeled as $PL(d_{i,u}) = (d_{i,u})^{\alpha_{i \to u}}$, where $d_{i,u}$ is the distance and $\alpha_{i \to u}$ is the path-loss exponent between the BS_i and U_u, respectively.

On the contrary, the link between the STAR-RIS, denoted by R, and each Base Station BS_i is assumed to exhibit a dominant line-of-sight (LoS) path [6]. Therefore, these links are subject to the Rician fading, where their channel coefficients are expressed as

$$\mathbf{h}_{i,R} = \sqrt{\frac{\rho_o}{PL(d_{i,R})}} \left(\sqrt{\frac{\kappa_{i,R}}{\kappa_{i,R} + 1}} \mathbf{v}_{\hat{i},R} + \sqrt{\frac{1}{\kappa_{i,R} + 1}} \mathbf{v}_{i,R} \right), \tag{2}$$

where $d_{i,R}$ is the distance between the BS_i and R, $\kappa_{i,R}$ represents the Rician factor, $\mathbf{v}_{\hat{i},R}$ represents the deterministic LoS components, and $\mathbf{v}_{i,R}$ denotes the complex Gaussian random variables, each following a Rayleigh distribution with zero mean and unit variance, thus representing the NLoS components. The links between R and U_u, $\forall u \in \mathcal{U}$, are also modeled in a similar fashion.

C. STAR-RIS Model

The energy splitting (ES) model of the STAR-RIS array can be mathematically characterized by the following respective transmission- and reflection-coefficient matrices [7]:

$$\mathbf{\Theta_r} = \sqrt{\beta^r} \text{diag}(e^{j\theta_1^t}, e^{j\theta_2^t}, \dots, e^{j\theta_K^t}), \tag{3}$$

$$\mathbf{\Theta_t} = \sqrt{\beta^t} \text{diag}(e^{j\theta_1^r}, e^{j\theta_2^r}, \dots, e^{j\theta_K^r}), \tag{4}$$

where β^t, $\beta^r \in [0, 1]$ and θ_k^t, $\theta_k^r \in [0, 2\pi)$, $\forall k \in \mathcal{K} \triangleq \{1, 2, \dots, K\}$. The phase shifts for transmission and reflection (i.e., θ_k^t and θ_k^r) can generally be chosen independently of each other [8]. However, the amplitude adjustments for transmission and reflection are coupled by the law of conservation of energy. Assuming the STAR-RIS does not impose any power loss, the relation between the amplitude coefficients (i.e., β^t and β^r) is expressed as $\beta^t + \beta^r = 1$. To reduce the signaling overhead between the STAR-RIS and the BSs, all elements are adjusted to have the same transmission and reflection coefficients.

III. PERFORMANCE ANALYSIS

A. Rates Analysis

To analyze the rates achieved for users in the system model shown in Fig. 1, we first present the signal model. Specifically, $\forall i \in \mathcal{I}, c \in \mathcal{C}, f \in \mathcal{F}$, let the tuple $(U_{1,c}, U_{2,c}, U_f)$ represent the coordinated NOMA cluster, and let P_1 and P_2 denote the transmit powers of BS_1 and BS_2, respectively. This signal model serves as the foundation for evaluating the achieved rates and optimizing the system performance in the considered cluster. Additionally, let $x_{1,c}, x_{2,c}$, and x_f represent the message signal intended for $U_{1,c}, U_{2,c}$, and U_f, respectively. Each BS_i broadcasts a superimposed signal of the messages [9] intended for users within its coverage region, $U_{i,c}$ and U_f, and expressed as:

$$x_i = \sqrt{\zeta_{i,c}P_i}x_{i,c} + \sqrt{\zeta_{i,f}P_i}x_f, \qquad (5)$$

where $\zeta_{i,c}$ and $\zeta_{i,f}$ are the power allocation (PA) factors assigned by BSi to users $U_{i,c}$ and U_f, respectively. It is important to note that $U_{i,c}$ experiences stronger channel conditions compared to U_f, making it the dominant NOMA user in the pair Ui, c, U_f formed by BSi. Following the principle of NOMA, Ui, c should be capable of detecting and decoding the message intended for U_f. This principle also implies that $\zeta_{i,c} < 0.5$, or $0.5 < \zeta_{i,f} < 1$ [10], [11].

For brevity, we only define the rate achieved by $U_{1,c}$ from the set of cell-center users $\mathcal{C}$, as the same steps could be extended to define the rate of $U_c, \forall c \in \mathcal{C}$. The received signal at $U_{i,c}$ can be written as:

$$y_{1,c} = \mathbf{h}_{1,c}x_1 + \mathbf{h}_{2,c'}x_2 + N_o, \qquad (6)$$

where N_o is an additive white Gaussian noise (AWGN), i.e., $N_o \sim \mathcal{CN}(0, \sigma^2)$. Further, $\mathbf{h}_{2,c'}$ is the channel corresponding to the link between BS_2 and $U_{1,c}$, which is the cell-center user of BS_1, and represents the ICI experienced at $U_{1,c}$. By utilizing successive interference cancellation (SIC) techniques, $U_{1,c}$ first decodes the message signal of U_f (i.e., x_f) and then removes it from $y_{1,c}$ to decode its own message (i.e., $x_{1,c}$). Based on this approach, the achievable rate at $U_{1,c}$ for decoding the message of U_f can be expressed as

$$\mathcal{R}_{1,c \to f} = \log_2\left(1 + \frac{\zeta_{1,f}P_1|\mathbf{H}_{1,c}|^2}{\zeta_{1,c}P_1|\mathbf{H}_{1,c}|^2 + P_2|\mathbf{h}_{2,c'}|^2 + \sigma^2}\right), \qquad (7)$$

where $\mathbf{H}_{1,c} = \mathbf{h}_{1,c} + \mathbf{h}_{R,c}^H\Theta_r\mathbf{h}_{1,R}$ represents the combined channel from BS_1 to $U_{1,c}$. Furthermore, the achievable rate at $U_{1,c}$ for decoding its own message can be expressed as:

$$\mathcal{R}_{1,c} = \log_2\left(1 + \zeta_{1,c}\frac{P_1|\mathbf{H}_{1,c}|^2}{P_2|\mathbf{h}_{2,c'}|^2 + \sigma^2}\right). \qquad (8)$$

On the contrary, U_f, belonging to two NOMA pairs, receives its signal through the broadcasts from each $BS_i, \forall i \in \mathcal{I}$. Thus, the received signal at U_f can be expressed as

$$y_f = \mathbf{H}_{1,f}x_1 + \mathbf{H}_{2,f}x_2 + N_0, \qquad (9)$$

where $\mathbf{H}_{1,f} = \mathbf{h}_{1,f} + \mathbf{h}_{R,f}^H\Theta_t\mathbf{h}_{1,R}$ and $\mathbf{H}_{2,f} = \mathbf{h}_{2,f} + \mathbf{h}_{R,f}^H\Theta_t\mathbf{h}_{2,R}$ denote the combined channels from BS_1 to U_f and from BS_2 to U_f, respectively. As we considered non-coherent JT-CoMP, the achievable rate at U_f can be expressed as [12], [13]:

$$\mathcal{R}_f = \log_2\left(1 + \frac{\zeta_{1,f}P_1|\mathbf{H}_{1,f}|^2 + \zeta_{2,f}P_2|\mathbf{H}_{2,f}|^2}{\zeta_{2,c}P_1|\mathbf{H}_{1,f}|^2 + \zeta_{2,c}P_2|\mathbf{H}_{2,f}|^2 + \sigma^2}\right), \qquad (10)$$

B. Problem Formulation

Based on the analysis conducted above, the joint network sum-rate optimization problem for a single coordinated NOMA cluster aided by STAR-RIS can be formulated as:

$$\max_{\mathcal{A},\Theta,\mathbf{K}_A} \quad \mathcal{R}_{sum} = \sum_{i=1}^{2}\mathcal{R}_{i,c} + \mathcal{R}_f \qquad (11)$$

$$\text{s.t.} \quad \mathcal{R}_f \geq R_{min}^f, \forall f \in \mathcal{F},$$
$$\mathcal{R}_{i,c} \geq R_{min}^{i,c}, \forall i \in \mathcal{I}, c \in \mathcal{C},$$
$$\zeta_{i,c}^2 + \zeta_f^2 \leq 1, \forall i \in \mathcal{I}, c \in \mathcal{C}, f \in \mathcal{F},$$
$$\theta_k^t \in [0, 2\pi), k \in \mathcal{K}$$
$$\theta_k^r \in [0, 2\pi), k \in \mathcal{K}$$
$$\beta_t + \beta_r = 1,$$
$$P_i \leq P_{max}^i, i \in \mathcal{I},$$

where R_{min}^f and $R_{min}^{i,c}$ represent the minimal achievable rates at U_f and $U_{i,c}$, respectively, and P_{min}^i is the maximum transmit power for each BS. In addition, $\mathcal{A}$ represents the PA factors of a single NOMA pair in the cluster, Θ represents all the phase shifts associated with STAR-RIS, and $\mathbf{K}_A$ is the splitting of STAR-RIS resources among the BSs.

As the CSI is fully estimated at the BSs, the optimal phase shift for each element $k \in \mathcal{K}$ can be computed [14], to solve the objective in 11 as follows:

$$\theta_k^p = \text{mod}[\arg(\mathbf{h}_{i,q}) - \arg(\mathbf{h}_{i,R} \cdot \mathbf{h}_{R,q}), 2\pi] \qquad (12)$$

where arg is the argument function and is utilized to compute the phase of the channels, $p \in \{t, r\}$ representing transmission and reflection regions of STAR-RIS, respectively, and $q \in \mathcal{C}$ when $p = t$, or $q \in \mathcal{F}$ when $p = r$. We adopt fixed empirical optimizations to address the joint network sum-rate optimization problem 11. Furthermore, we analyze the impact of distributing the STAR-RIS elements among the BSs by systematically exploring all conceivable splitting configurations through an exhaustive iteration process.

Advanced optimization techniques could potentially offer further improvements. However, the primary focus of this work is to showcase the fundamental enhancements attained by strategically deploying the STAR-RIS and distributing its resources among the Base Stations (BSs) within the coordinated NOMA cluster.

IV. NUMERICAL RESULTS

This section presents numerical results for assessing the STAR-RIS enhancements in the proposed coordinated NOMA cluster.

A. Simulation Setup

We consider an outdoor environment where the transmission bandwidth of the network is set to $B = 1$ MHz, and the power of AWGN is set to $\sigma^2 = -174 + 10\log_{10}(B)$ (dBm) with a noise figure N_F of 12 dB. For simplicity, we assume that the transmit powers of both BS_1 and BS_2 are identical, expressed as $P_1 = P_2 = P_t$. Moreover, the PA factors for $U_{1,c}$, $U_{2,c}$, and U_f are fixed to $\zeta_{1,c} = \zeta_{2,c} = 0.3$ and $\zeta_f = 0.7$, respectively.

In the three-dimensional Cartesian coordinate system, the locations of BS_1 and BS_2, each with a coverage radius of 60 m, are set to (-50m, 0m, 25m) and (50m, 0m, 25m) respectively. The STAR-RIS is strategically placed at the intersection of the two cells, near U_f, specifically, at the coordinates (0m, 25m, 5m). Additionally, the cellular users U_1,c, U_2,c, and U_f are positioned at (-40m, 18m, 1m), (30m, 22m, 1m), and (0m, 35m, 1m), respectively. Some specific parameters used for simulation are outlined in Table I.

TABLE I
SIMULATION PARAMETERS

Parameters	Values
Path-loss exponent of BS_i-U_c links	$\alpha_{i \to c} = 3$
Path-loss exponent of BS_i-U_f link	$\alpha_{i \to f} = 3.5$
Path-loss exponent BS_i-RIS links	$\alpha_{i \to R} = 3$
Path-loss exponent of RIS-U_c links	$\alpha_{R \to c} = 2.7$
Path-loss exponent of RIS-U_f link	$\alpha_{R \to f} = 2.3$
Path-loss exponent of Interfering links	$\alpha_{i \to c'} = 4$
Rician factor of RIS-U_c links	$\kappa_{R \to c} = 4$ dB
Rician factor of RIS-U_f link	$\kappa_{R \to f} = 3$ dB

B. Impact of the Number of STAR-RIS Elements

The outage probabilities and achievable rates for each user in the cluster are presented in Fig. 2 and Fig. 3, respectively. With an increase in the number of elements K, we observe a notable reduction in outage probability of the cell-edge user U_f. This improvement is attributed to the enhanced data coverage facilitated by the STAR-RIS [15]. Note that outage probabilities of $U_{1,c}$ and $U_{2,c}$ do not experience any substantial improvements, as their links are already dominated by the near base station BS_1 and BS_2, respectively. Moreover, due to strong ICI experienced by U_f in the non-CoMP configuration, it experiences high outage probabilities, for all transmission power levels. The same trend is observed in the evaluation of user rates, with higher numbers of STAR-RIS elements leading to improved user rates.
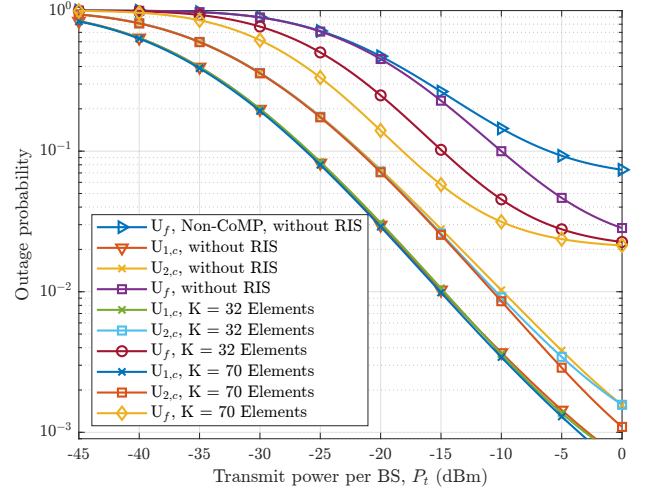

Fig. 2. Outage probability of all the users (U_{1c}, U_{2c}, U_f) versus P_t, where $\beta^t = 0.5$ and $\beta^r = 0.5$ when $K > 0$.
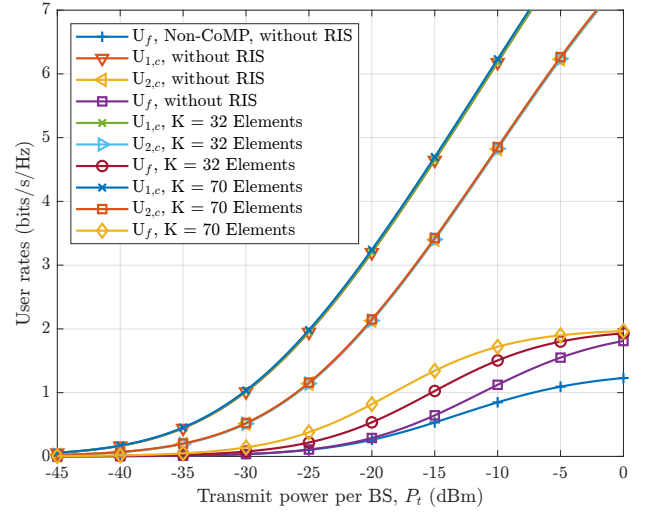

Fig. 3. Achievable rate of both the center users (U_{1c}, U_{2c}) and edge user U_f versus P_t with different STAR-RIS settings.

C. Coordinated NOMA Power Allocation Factors

The impact of PA factors in the coordinated NOMA cluster is evaluated in Fig. 4. The optimization problem of PA factors in a NOMA pair is formulated as follows:

$$\max_{\mathcal{A}} \quad \mathcal{R}_{i,c} + \mathcal{R}_f \qquad (13)$$
$$\text{s.t.} \quad \zeta_{i,c}^2 + \zeta_f^2 \leq 1, \forall i \in \mathcal{I}, c \in \mathcal{C}, f \in \mathcal{F},$$

Following the methodology proposed in [16], we obtain the optimal PA factors, denoted as ($U_{1,c}$, Uf) and ($U2, c$, U_f). For the purpose of assessing the impact of power allocation factors on top of the STAR-RIS enhancements, we specifically focus on the case for a configuration with $K = 70$ elements. Notably, this configuration yields the highest network sum-rate among all considered cases.
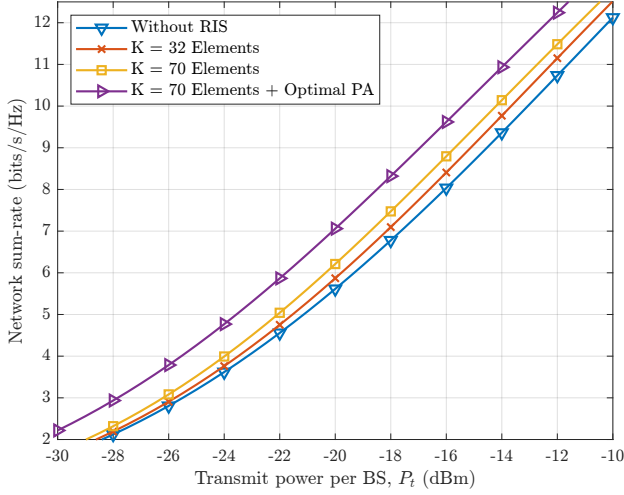
Fig. 4. Achievable network sum-rate versus P_t, where $\beta^t = 0.5$ and $\beta^r = 0.5$ when $K > 0$.

D. Exhaustive STAR-RIS Element Allocation

By performing exhaustive iterations over all potential combinations of STAR-RIS element assignments to BS_1 and BS_2 in one dimension and exploring various transmission and reflection amplitude adjustments (β_t and β_r) in another dimension, with $P_t = -15$ dBm, we plot the network sum-rate as a function of said dimensions. As evident from Fig. 5, the network sum-rate peaks when $\beta_t > \beta_r$. This observation aligns with the expectations, considering that the STAR-RIS is strategically positioned near U_f, located in the transmission region Θ_t, thereby leading to an optimal network sum-rate.

E. Spectral Efficiency & Energy Efficiency Trade-off

In Figure 6, we present the evaluation of the trade-off between spectral efficiency (SE) and electrical efficiency (EE). At circuit power $P_{\text{circuit}} = 1$ mW and the optimal operating
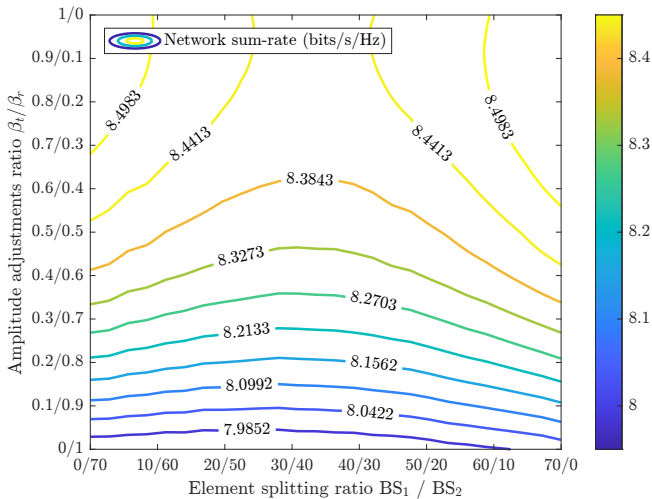

Fig. 5. Contour plot of network sum-rate as a function of STAR-RIS element allocation to BSs and amplitude adjustments (β^t, β^r) for $P_t = -15$ dBm.

point, it is evident that the CoMP-NOMA cluster assisted by STAR-RIS, with a larger number of elements K, achieves the highest EE. This observation can be attributed to the passive nature of STAR-RIS elements, which enhance the effective channel between the BSs and users by leveraging phase shifts, consequently resulting in a higher achievable network sum-rate.
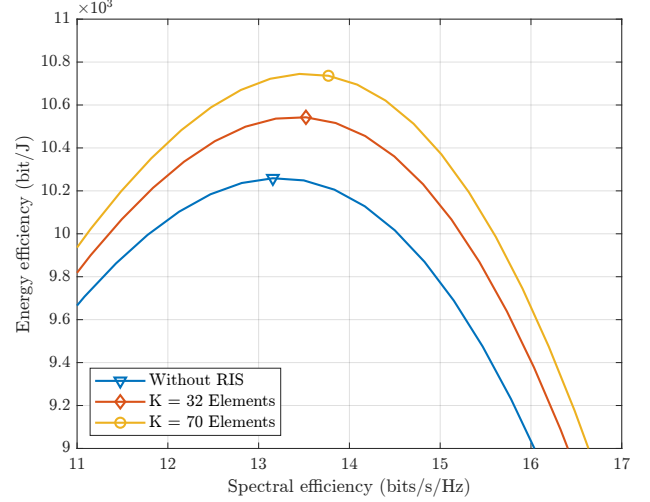

Fig. 6. SE and EE trade-off for a different number of STAR-RIS elements.

V. CONCLUSION

In this paper, we present a novel approach for STAR-RIS COMP NOMA networks, aiming to maximize data rates and improve outage conditions for all cellular users. By thoroughly optimizing STAR-RIS resources, this study effectively harnesses the synergies between STAR-RIS and CoMP-NOMA networks, resulting in elevated data rates and expanded data coverage. An essential aspect of our investigation is including the cell-edge user within NOMA pairs formed by each BS, leading to higher diversity gains. The outcomes of this study pave the way for potential future research directions, including exploring the proposed approach's scalability and adaptability to large-scale networks and diverse communication scenarios. Moreover, considering advanced optimization techniques, such as deep reinforcement learning, to address resource allocation challenges offers another promising avenue for future research endeavors.

REFERENCES

[1] Q. Wu and R. Zhang, "Towards smart and reconfigurable environment: Intelligent reflecting surface aided wireless network," *IEEE communications magazine*, vol. 58, no. 1, pp. 106–112, 2019.
[2] M. Di Renzo, A. Zappone, M. Debbah, M.-S. Alouini, C. Yuen, J. De Rosny, and S. Tretyakov, "Smart radio environments empowered by reconfigurable intelligent surfaces: How it works, state of research, and the road ahead," *IEEE journal on selected areas in communications*, vol. 38, no. 11, pp. 2450–2525, 2020.
[3] T. Hou, J. Wang, Y. Liu, X. Sun, A. Li, and B. Ai, "A joint design for star-ris enhanced noma-comp networks: A simultaneous-signal-enhancement-and-cancellation-based (ssecb) design," *IEEE Transactions on Vehicular Technology*, vol. 71, no. 1, pp. 1043–1048, 2021.

[4] L. Wei, C. Huang, G. C. Alexandropoulos, C. Yuen, Z. Zhang, and M. Debbah, "Channel estimation for ris-empowered multi-user miso wireless communications," *IEEE Transactions on Communications*, vol. 69, no. 6, pp. 4144–4157, 2021.

[5] A. Taha, M. Alrabeiah, and A. Alkhateeb, "Enabling large intelligent surfaces with compressive sensing and deep learning," *IEEE access*, vol. 9, pp. 44304–44321, 2021.

[6] Y. Guo, Z. Qin, Y. Liu, and N. Al-Dhahir, "Intelligent reflecting surface aided multiple access over fading channels," *IEEE Transactions on Communications*, vol. 69, no. 3, pp. 2015–2027, 2020.

[7] X. Mu, Y. Liu, L. Guo, J. Lin, and R. Schober, "Simultaneously transmitting and reflecting (star) ris aided wireless communications," *IEEE Transactions on Wireless Communications*, vol. 21, no. 5, pp. 3083–3098, 2021.

[8] J. Xu, Y. Liu, X. Mu, and O. A. Dobre, "Star-riss: Simultaneous transmitting and reflecting reconfigurable intelligent surfaces," *IEEE Communications Letters*, vol. 25, no. 9, pp. 3134–3138, 2021.

[9] Y. Saito, Y. Kishiyama, A. Benjebbour, T. Nakamura, A. Li, and K. Higuchi, "Non-orthogonal multiple access (noma) for cellular future radio access," in *2013 IEEE 77th vehicular technology conference (VTC Spring)*, pp. 1–5, IEEE, 2013.

[10] M. Obeed, H. Dahrouj, A. M. Salhab, S. A. Zummo, and M.-S. Alouini, "User pairing, link selection, and power allocation for cooperative noma hybrid vlc/rf systems," *IEEE Transactions on Wireless Communications*, vol. 20, no. 3, pp. 1785–1800, 2020.

[11] A. Salem and L. Musavian, "Noma in cooperative communication systems with energy-harvesting nodes and wireless secure transmission," *IEEE Transactions on Wireless Communications*, vol. 20, no. 2, pp. 1023–1037, 2020.

[12] R. Tanbourgi, S. Singh, J. G. Andrews, and F. K. Jondral, "A tractable model for noncoherent joint-transmission base station cooperation," *IEEE Transactions on Wireless Communications*, vol. 13, no. 9, pp. 4959–4973, 2014.

[13] M. Elhattab, M. A. Arfaoui, C. Assi, and A. Ghrayeb, "Ris-assisted joint transmission in a two-cell downlink noma cellular system," *IEEE Journal on Selected Areas in Communications*, vol. 40, no. 4, pp. 1270–1286, 2022.

[14] Q. Wu and R. Zhang, "Intelligent reflecting surface enhanced wireless network via joint active and passive beamforming," *IEEE transactions on wireless communications*, vol. 18, no. 11, pp. 5394–5409, 2019.

[15] T. Wang, M.-A. Badiu, G. Chen, and J. P. Coon, "Outage probability analysis of star-ris assisted noma network with correlated channels," *IEEE Communications Letters*, vol. 26, no. 8, pp. 1774–1778, 2022.

[16] F. Fang, H. Zhang, J. Cheng, and V. C. Leung, "Energy-efficient resource allocation for downlink non-orthogonal multiple access network," *IEEE Transactions on Communications*, vol. 64, no. 9, pp. 3722–3732, 2016.